www.advmattechnol.de

Nature-Inspired Anti-Reflective Texturization for Solar Energy Applications

Anastasia Novikova, Aviad Katiyi, and Alina Karabchevsky*

Solar energy is a source of renewable energy that is harnessed using a range of technologies. With the development of humanity's interest in solar energy, there is a need to collect and store it. However, the current photovoltaic cells that are used to collect solar energy are far from being optimized, and their further development is in much demand. While there are many factors related to the low efficiency of solar cells, the main challenge is in solving optical losses. In this review, a comprehensive overview of texturization as occurring in nature is provided and recently reported as a technique to increase the transparency of surfaces. The basic concepts and typical patterns are introduced, followed by a discussion of representative works and their uniqueness. Furthermore, insights regarding the future of the emerging domain of nature-inspired anti-reflective patterns, with the goal of encouraging researchers to enhance solar cell efficiency and expand the utilization of such patterns for various applications are presented.

1. Introduction

Since the beginning of the industrial era, energy has been derived from fossil-based materials such as coal and oil. During the burning process, pollutants are emitted into the environment; for example, heavy metals, radionuclides, benzopyrenes, and numerous other substances. [1-3] In recent decades, the world has been moving toward green energy sources produced from natural resources, such as solar, wind, and hydroelectric power. For example, wind power can be converted by wind turbines, and hydroelectric power by building a dam in a river. These sources are clean and do not involve a burning process which would emit pollutants into the environment. One of the most promising renewable energy sources is solar energy, which is based on the sun's radiation. Solar energy does not pollute the environment and is

A. Novikova, A. Katiyi, A. Karabchevsky School of Electrical and Computer Engineering Ben-Gurion University of the Negev Beer-Sheva 8410501, Israel E-mail: alinak@bgu.ac.il

The ORCID identification number(s) for the author(s) of this article can be found under https://doi.org/10.1002/admt.202301128

© 2023 The Authors. Advanced Materials Technologies published by Wiley-VCH GmbH. This is an open access article under the terms of the Creative Commons Attribution-NonCommercial-NoDerivs License, which permits use and distribution in any medium, provided the original work is properly cited, the use is non-commercial and no modifications or adaptations are made.

DOI: 10.1002/admt.202301128

a promising advance, as technologies for collecting and storing energy are still being developed. In solar cells, the photovoltaic effect is utilized for converting photons to electrons. A photon that matches the energy gap of the material is absorbed and converted into an electron. The energy gap is defined by the material and the doping which define the quantum efficiency. The photovoltaic effect was first observed in 1839 by Edmond Becquerel,[4] who found that two brass plates immersed in liquid under sunlight provided current. In 1883, Charles Fritts developed the first solar cell by coating selenium with a thin layer of gold. It achieved an efficiency of 1-2%. Later, in 1954, a single crystal silicon solar cell demonstrated by Bell Labs achieved an efficiency of 6%.^[5] Since then,

commercial solar cells have achieved an efficiency of 15–20%, while researchers have achieved $\approx 50\%$ efficiency. Currently, solar cells are becoming very common in homes and even in industries.

One of the solar cell challenges needing to be addressed is that of the partially reflected incident light, which harms their efficiency. As light hits the boundary of two materials, the power is split and a fraction of the power is refracted. As the index contrast between the materials increases, the reflection increases and can achieve high values. The reflectance can be calculated by Fresnel's equations. For example, in the case of a silicon-air surface, 35% of the light can be reflected. [6] Various methods can be used to address this issue. The common method for reducing reflections is by coating the surface with an anti-reflection (AR) layer. The anti-reflection layer is made of a single thin layer of transparent material with a refractive index equal to the square root of the substrate refractive index. By decreasing the refractive index contrast between the mediums, the reflection, which can be calculated by Fresnel's equation, is reduced. The anti-reflection coating can be achieved by using a variety of materials such as mesoporous silica nanoparticles on polymer substrate, [7] zircon and its oxides, [8] and magnesium fluoride. [9] An improvement in this method of achieving anti-reflection properties is by using multilayers. The coating layer can be composed of two layers with the same or different thicknesses on a substrate.[10,11] When more than two layers are applied to the surface, it is possible to create more combinations of materials, which makes it easier to reduce the reflection.[12-14] Layer coating methods are very

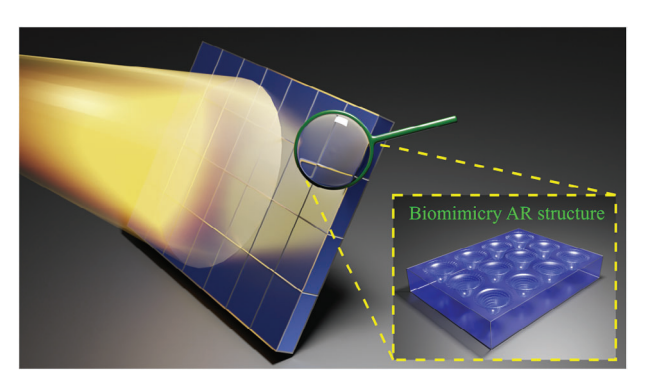


Figure 1. Illustration of biomimicry anti-reflection structure engraved on a solar cell

effective but are band-limited and are also limited by the selection of the material.

In addition to the above methods, porous materials are used to obtain anti-reflective surfaces. Since silicon is the primary material used in current solar panels, most research on porous structures focuses on silicon materials. They are processed mainly by chemical, [15] electrochemical, [16] and dry etching. [17] Chemical etching has been a long-standing method for achieving reflective surfaces, commonly employed in manufacturing due to its simplicity and effectiveness in surface treatments. However, this process typically involves the use of potent reagents, which pose environmental risks.

A new and promising method for anti-reflection is by modifying the surface of the material with sub-wavelength structures, as illustrated in **Figure 1**. By fabricating sub-wavelength structures, the properties of the material can be changed without involving other materials in the reflection-reducing process. It overcomes the limitations of the layer coating method mentioned above and has flexibility in the fabrication process. In this paper, we present methods and materials for anti-reflection sub-wavelength structures. In addition, we will discuss future directions for decreasing reflection, based on the nature of biomimicry.

First, we will briefly describe the fundamentals of subwavelength structures, such as sub-wavelength gratings and metamaterials. "Metamaterial" comes from Greek and means "beyond material." It includes artificial materials that do not exist in nature, such as a negative refractive index.[18] In subwavelength structures, the unit structure is significantly smaller than the incident wavelength and can be periodic or non-periodic. It allows the changing of the properties of materials and control of light at the nanoscale, and can be 1D, 2D, or 3D. The first observed sub-wavelength structure in optics, dated back to 1962, was the moth-eye. [19] Sub-wavelength structures are of growing interest in a variety of applications, such as wire grid polarizers, [20,21] waveguide grating couplers, [22,23] and invisibility cloaking.[24] Sub-wavelength structures can also be utilized for anti-reflection. As light hits the boundary of two materials, a fraction of the power is reflected. The amplitude refraction coefficient for a normal incident angle can be calculated by Fresnel's equations

$$R = \left(\frac{n_1 - n_2}{n_1 + n_2}\right)^2 \tag{1}$$

where n_1 and n_2 are the refractive indices of the materials. It shows that as the refractive index contrast between the materials increases, the reflection increases. For example, in siliconair boundary in visible light ($\lambda = 380-750^{\circ}$ nm), silicon has a high refractive index ($n_{Si} = 6.58-3.71$) and the reflection is in the range of R = 0.541-0.33. Therefore, creating an anti-reflection coating is of great importance for silicon-based devices in general and solar cells in particular. Sub-wavelength structures can be utilized for changing the refractive index to decrease the reflection and, therefore, increase the efficiency. In 1950, Rytov showed theoretically that a sub-wavelength structure with a period much smaller than the wavelength behaves as an equivalent homogeneous material with an equivalent refractive index, depending on the thickness of the layers. [25] Assuming incident light is normal to the structure for light polarization parallel (n_{\parallel}) or perpendicular (n_{\perp}) , the effective refractive index is defined as:

$$n_{\parallel}^{2} = f n_{1}^{2} + (1 - f) n_{2}^{2} \tag{2}$$

$$n_1^{-2} = f n_1^{-2} + (1 - f) n_2^{-2}$$
(3)

where *n* is the refractive index and $f = a/\Lambda$ is the duty cycle of the first medium, where a is the thickness of the first medium (n_1) and Λ is the period length. This shows that by changing the thickness of the materials, different refractive indices can be produced. It is worth noting that Rytov formulations can give a good starting point, but for a more accurate solution, numerical analysis is needed. Sub-wavelength structures can be utilized for creating gradient refractive index (GRIN), where the refractive is gradually increased from air to the material, which in turn reduces the reflection.^[26] The multilayer method may also achieve GRIN coating but has a few limitations—as presented abovethat make this process very challenging. Sub-wavelength structures eliminate those limitations and can create a smooth GRIN coating by milling inclusions or fabricating structures from only one material. In addition, there is a lot of freedom in designing and fabricating sub-wavelength structures. The structures can be of different shapes (spherical, cylindrical, conical, and cubic, etc.[27-30]), and from various materials (dielectric, copper, titanium dioxide, and silver, etc.[31-35]); and various refractive index profiles of gradient layers can be produced (such as linear, parabolic, cubic, Gaussian, fifth, exponential, sinusoidal, and Klopfenstein coverage^[36–38]). We have drawn inspiration from the anti-reflective properties found in jellyfish eyes to develop a synthetic anti-reflective surface on the waveguide facets.^[39,40] This innovation aimed to enhance the transparency of waveguides in the near-infrared spectrum. Our research has led to the creation of an optimized metamaterial with unit cells measuring 560 × 560 nm, resulting in a remarkable 2.6-fold improvement in transparency compared to waveguides lacking this surface modification. To achieve this, we employed a focused ion beam to engrave metasurfaces onto the waveguide facets. Our experiments involved testing these silicon-on-insulator waveguides using an inline setup. The far-field scattering patterns we observed demonstrated that the unique geometry of the unit cells in the engraved metamaterial played a crucial role in achieving this remarkable effect. This effect can be attributed to directional scattering, leading to a dual outcome: first, the device achieved

-and-conditions) on Wiley Online Library for rules of use; OA articles are governed by the applicable Creative Commons

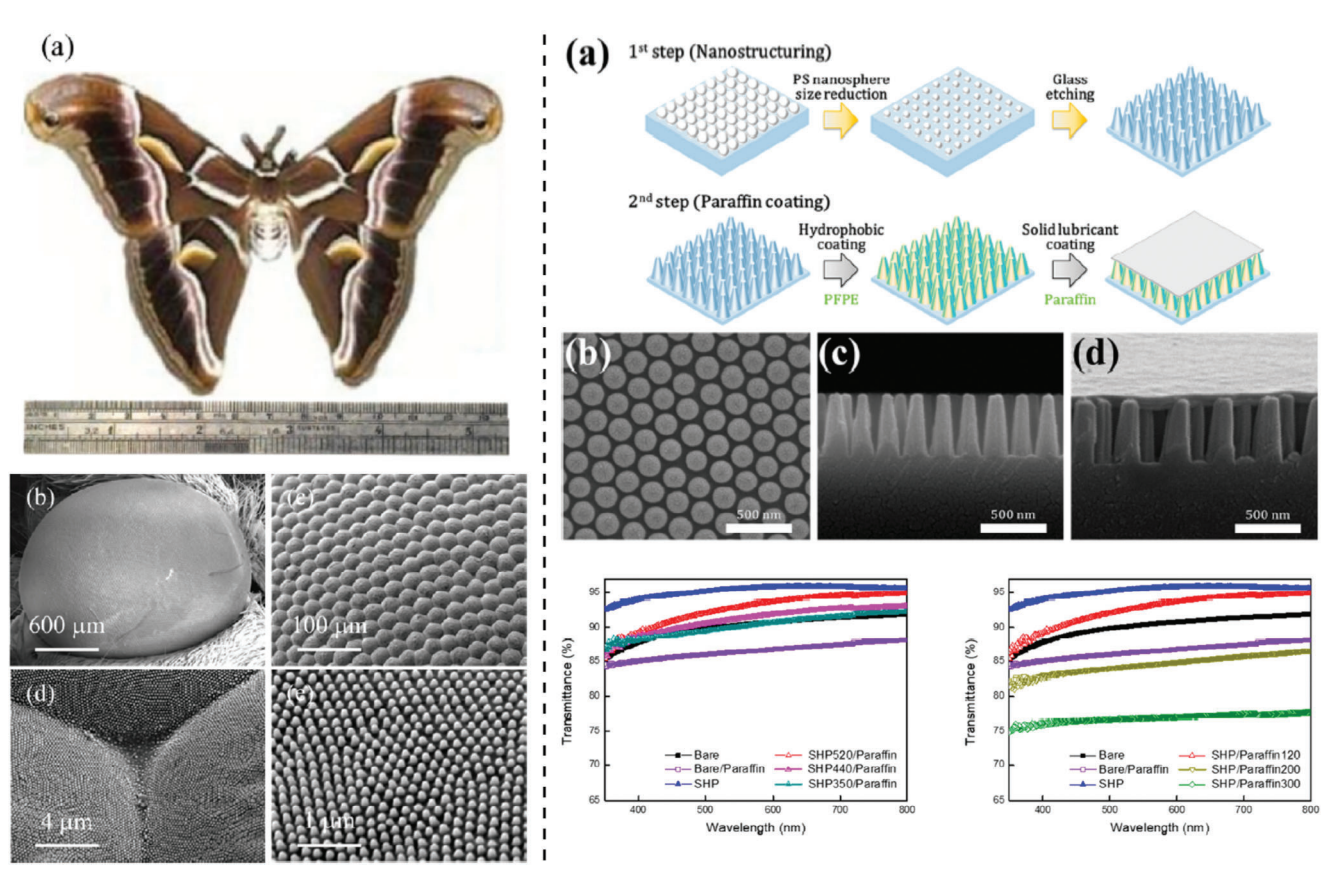


Figure 2. (Left) Image of *Philosamia cynthia ricini* moth and scanning electron microscope (SEM) images of the structure of a moth eye. Reproduced with permission.^[67] Copyright 2016, American Chemical Society. (Right) Moth eye-inspired surfaces. a) Illustration of the fabrication process. b–d) SEM images of the fabricated structures and experimental results for moth-eye inspired anti-reflection coating. Reproduced with permission.^[68] Copyright 2020, American Chemical Society.

exceptionally high transparency, and second, it efficiently coupled with low-order modes thanks to the focusing properties of the dielectric nano-antennas. This breakthrough in creating waveguide facets with anti-reflective metamaterials on a microchip opens up new avenues for engineering transparent on-chip devices with superior coupling efficiency. These applications span a wide range, from sensing technologies to advancements in quantum technologies. [41] Sub-wavelength structures have already found applications as anti-reflective surfaces. Table 1 presents the most widespread structures currently in use, with a brief description of their production technologies and materials.

2. Anti-Reflecting Sub-Wavelength Structures

One of the methods to reduce the reflection from a material is by modifying its surface using sub-wavelength surfaced-textured structures^[60–62] such as porous layers.^[63–66] The effectiveness of porous structures depends on several parameters, such as pore size, porous surface thickness, and porosity density. The pore size should be many times smaller than the wavelength of light and the refractive index of a nanoporous surface is obtained by averaging over the entire surface. The refractive gradient of a silicon wafer depends on the thickness of the film and the density of the

porous material. The texturing process is either the application of pyramidal or cone-shaped arrays to the surface or the application of 2D grooves equal to half the wavelength. The textured surface also exhibits anti-glare properties at wavelengths much smaller than the characteristic texture size. This is due to the fact that the rays initially reflected from the textured surface are likely to penetrate the medium during subsequent re-reflections from irregularities. At the same time, texturing the surface creates conditions under which a passing beam can deviate from the normal incidence, which leads to the effect of "entanglement of passing light."

Recently, inspired by natural animal features, researchers have designed artificial anti-reflection structures with different properties and wavelength ranges. Below, we will describe the sub-wavelength structures that are already in use.

2.1. Moth Eyes

The first nature-inspired structure for anti-reflection was a moth eye, as shown in **Figure 2**. The moth eye was the first observation of a sub-wavelength structure in optics. In 1962, a sub-wavelength structure of spaced pillars, or "corneal nipples," was

onditions) on Wiley Online Library for rules of use; OA articles are governed by the applicable Creative Commons License

Table 1. Sub-wavelength texturization.

The structure	Methods of obtaining	Materials	Ref.
Jellyfish eyes	Focused ion beam	Silicon	[40]
Moth eyes	holographic lithography,	Au nanocluster,	[42-45]
	laser, use of masks, embossing	SiO ₂ films, Cr	
	nano print	nanospheres	
Leafhopper brochosomes	Colloidal deposition, etching	silica nanospheres	[46–49]
		with gold, WO3, NiO	
Dragonfly wings	Colloidal lithography,	silica, polymer	[50–52]
	holography lithography		
	nano print		
Clear wings butterfly	Holographic lithography,	nanostructured	[53–55]
	laser, use of masks, embossing,	glass	
	nano print		
Chitin nanofiber	Extraction of pure chitin	Chitin	[56–59]

seen in the corneas of night-flying moths, by the use of scanning electron microscopy. [19] Moth eyes have an unusual property: their surfaces are covered with a natural nanostructured film that eliminates reflections. The nano-structures allow the moth to see clearly in the dark, without reflections that can give away its location to predators. The structure is made of a hexagonal pattern

of irregularities, each approximately 200 nm high and spaced 300 nm apart in the center. [69] This kind of anti-reflection coating works because the roughness is smaller than the wavelength of visible light, so light "sees" the surface as a continuous gradient refractive index between air and medium, which reduces reflection, effectively removing the air-lens interface. In 1967,

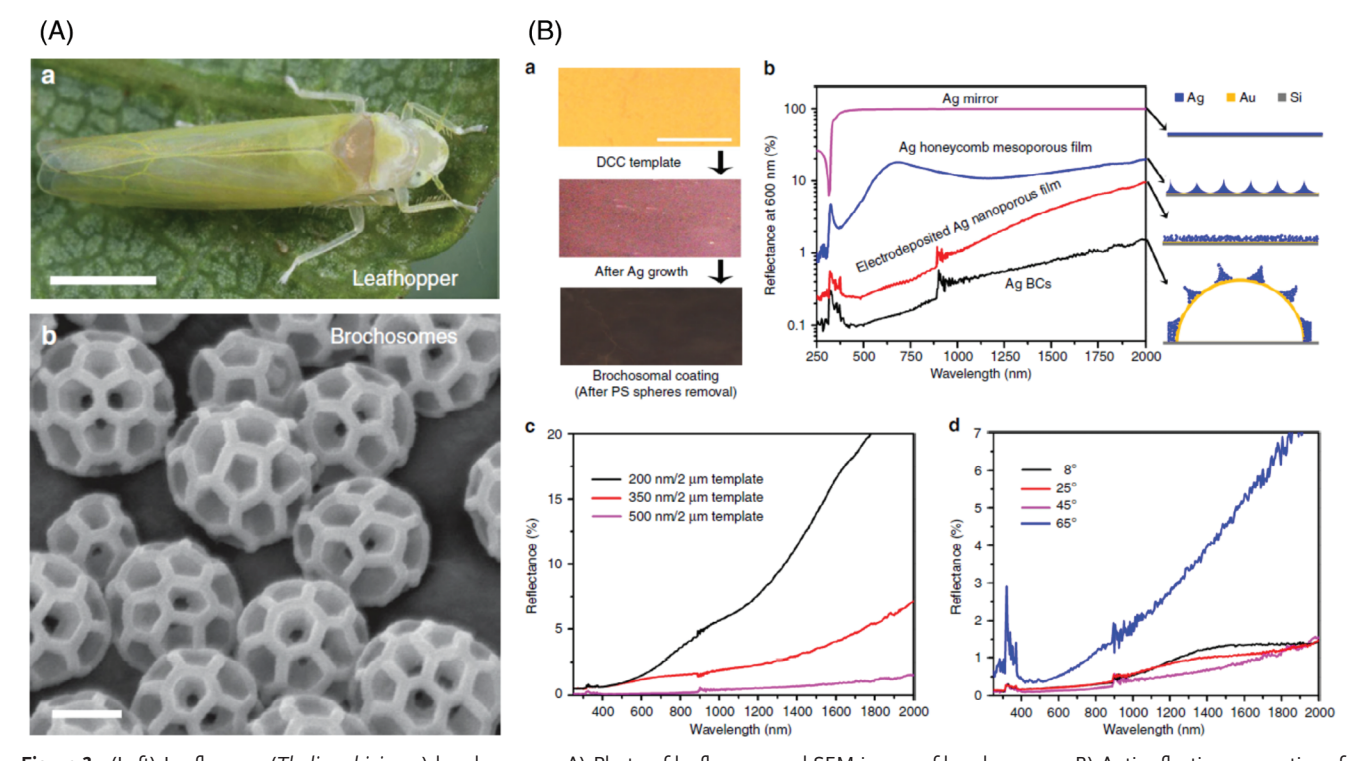


Figure 3. (Left) Leafhopper (*Thalia rubiginosa*) brochosomes. A) Photo of leafhopper and SEM image of brochosomes. B) Anti-reflection properties of synthetic brochosomes. (Right) a) Images at different steps of the process. b) Reflection of Ag mirror, Ag honeycomb mesoporous film, Ag nanoporous film, and Ag BCs. c,d) Reflectance of different pit sizes and incident angle. Reproduced with permission.^[75] Copyright 2017, Springer Nature.

and-conditions) on Wiley Online Library for rules of use; OA articles are governed by the applicable Creative Common

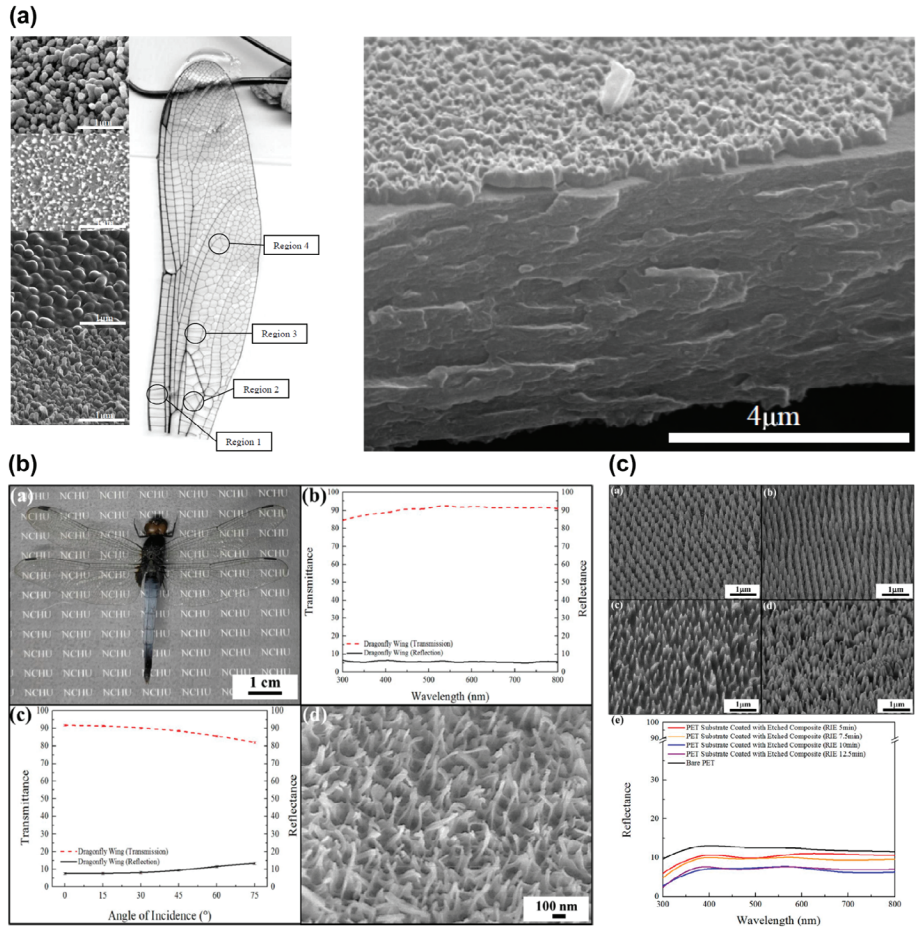


Figure 4. a) Scanning electron microscope images of dragonfly (*Aeshna cyanea*) wings nanostructures in different regions of the wing and a cleaved section of a single wing membrane. Reproduced with permission.^[77] Copyright 2006, Optica Publishing Group. b) Anti-reflection properties of a blue-tailed forest hawk dragonfly (*Orthetrum triangulare*) wings and c) wing-inspired conical structures with different oxygen and argon RIE treatment. Reproduced with permission.^[84] Copyright 2020, American Chemical Society.

Bernhard discovered the anti-reflection property of the moth.^[70] He proposed that the reduction of the reflection was caused by the gradual refractive index change between air and cornea due to the eye structure. A few years later, the structure of the moth eye was analyzed using an electron microscope, and an artificial moth eye was fabricated on a lens to reduce reflection.^[71] In 2008, a moth eye anti-reflection coating was applied to silicon.^[43] Using a monolayer silica colloidal crystal-polymer nanocomposite and a few etching processes, a broadband anti-reflection coating structure was formed on silicon, decreasing the reflection to below 2.5%. Anti-reflection films inspired by the moth eye structure have, since then, been fabricated for use in decreasing the reflection in solar cells.^[32,36,72-74]

2.2. Leafhopper (Thalia rubiginosa) Brochosomes

Along the evolutionary process, insects have evolved highly transparent wings to avoid predators.^[76,77] One of the new directions of research in the field of sub-wavelength structures based on biomimicry is the study of the wings of the Leafhopper (*Thalia*

rubiginosa). The wings of this insect exhibit anti-glare behavior at wide viewing angles as a result of chromosomal coatings transferred by leaf wrappers on the wing surface, as shown in Figure 3. Leafhopper brochosomes are microscopic granules of complex structure with a honeycomb pattern that resembles a soccer ball.[78] Leafhoppers from different areas will produce brochosomes with different geometries and properties.^[79] They are usually found on the surface of the body and, less often, on egg clusters.^[79] The embroidered ball-like brochosomes establish a gradual transition in the refractive index at the air/wing interface, leading to broadband omnidirectional anti-reflection performance. In 2017, artificial brochosome-inspired coatings were fabricated using double-layer colloidal crystal templates combined with site-specific electrochemical growth.^[75] An ultra anti-reflection from 250 to 2000 nm with an average reflection of less than 1% was achieved. Inspired by brochosomal coatings, this study develops a non-photolithography-based approach for assembling embroidered ball-like structure arrays, exploiting a modified Langmuir-Blodgett technology.[47] The average visible transmittance of a polymer film can be improved by 8% at normal incidence, and improved by even 24% as the

. (https://onlinelibrary.wiley.com/terms-and-conditions) on Wiley Online Library for rules of use; OA articles are governed by the applicable Creative Commons

nically with nipple height at a

C

b

Arant. The reflectance, however, depend

larization when the angle of incidence is

gure 7a,b show how the reflectance for 500

pends on the angle of incidence for differen

3 cm

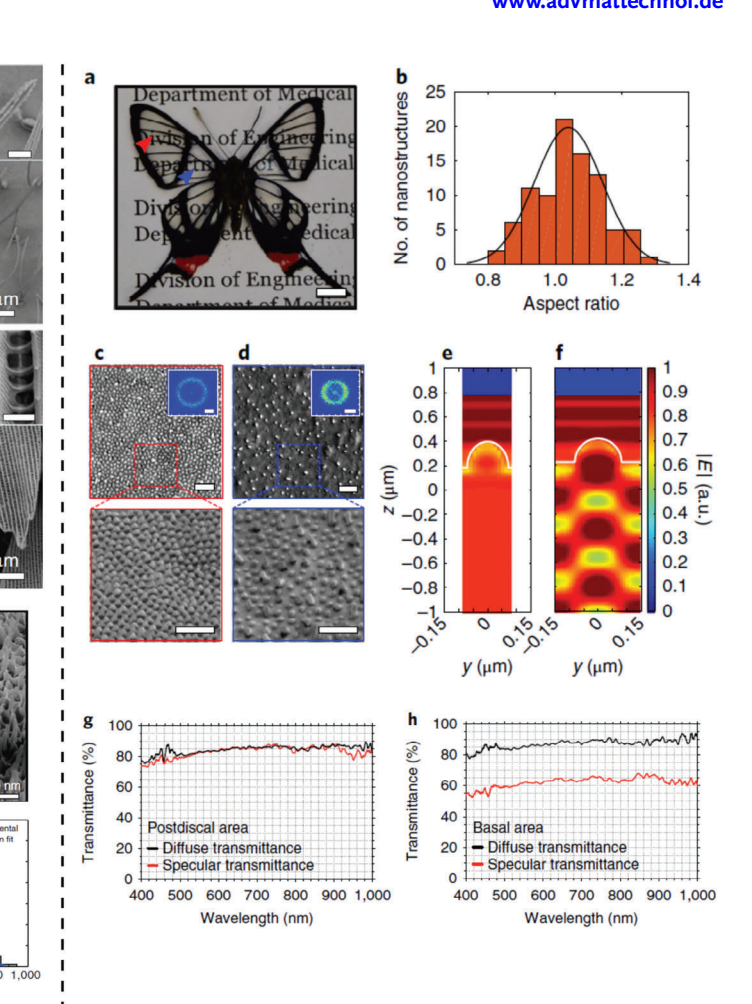


Figure 5. (Left, top) Glasswing butterfly. A) Image and B–D) SEM images of glasswing butterfly with the aspect ratio distribution of the dome-shaped nanostructures. (Left, bottom) a–e) SEM images of the anti-reflection nanostructures of the glasswing and f) the aspect ratio distribution. Reproduced with permission.^[88] Copyright 2015, Springer Nature. (Right) Longtail glasswing butterfly. a) Image of longtail glasswing butterfly. b) The aspect ratio distribution of the dome-shaped nanostructures. c,d) SEM images of the nanostructures, and e,f) FDTD numerical simulation. g,h) Transmittance of the nanostructures. Reproduced with permission.^[89] Copyright 2018, Springer Nature.

incident angle reaches 75° , by introducing the artificial brochosome arrays. The dependence of the structural shape on the anti-reflection capabilities is also systemically studied in this research.[80–83]

2.3. Dragonfly Wings

Another insect with wings that inspired anti-reflection structures is the dragonfly. The wing pattern is a randomly arranged irregular conical structure for a different region of the wing^[77] as shown in **Figure 4a**. The structure of the dragonfly wing is composed of wax-coated irregular structures, covering transparent membranes consisting of a cuticular layer. For example, a blue-tailed forest hawk dragonfly (*Orthetrum triangulare*) has randomly inclined conical structures which can achieve an average of 91% transmittance with a decrease of only 6% for the angle of 75° (Figure 4b).^[84] In their work, the authors use conical structures with tips based on a shape memory polymer. The structures provide a gradual transition of the refractive index to

the suppression of optical reflection in the visible spectrum, as shown in Figure 4c. Another interesting feature of this work is that the configuration of the structures is controlled by pressure, temperature, and solvent exposure. The resulting characteristics of the unidirectional and omnidirectional coatings can be instantly and reversibly switched. [85–87] Such structures capable of switching have a great potential for use in smart homes, and specifically for smart windows, for both energy collection and reflection.

2.4. Clear Wing Butterfly

Numerous species of butterflies have transparent glass-like wings. The wings have a sub-wavelength structure similar to one of the variants of the moth eye. However, in butterfly wings, the structures are more disordered and have varying dimensions, as can be seen in **Figure 5**. Different clear wing butterflies have different anti-reflection structures. A glasswing butterfly (*Greta oto*) has wings composed of nanopillars with a high aspect

.com/terms-and-conditions) on Wiley Online Library for rules of use; OA articles are governed by the applicable Creative Commons

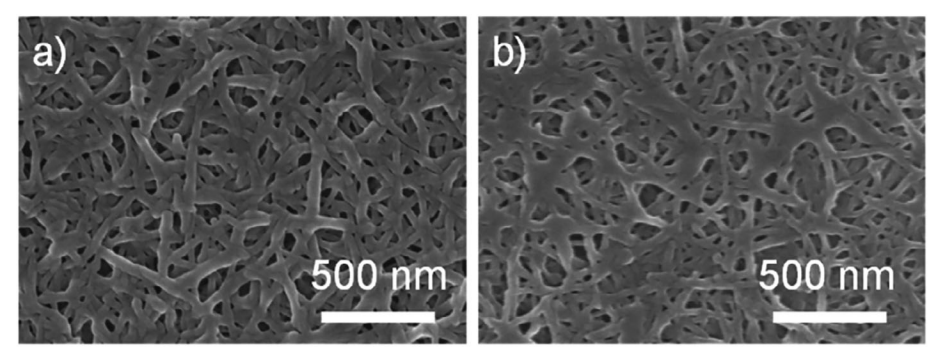


Figure 6. SEM images of chitin nanofibers a) before and b) after abrasion tests. Reproduced with permission. [61] Copyright 2016, American Chemical Society.

ratio (typically 5 but can reach 10)[88] as shown in Figure 5 (left). The structure was investigated and numerically simulated for anti-reflection behavior. [88] It was found that the randomness of the size and the distribution of the nanopillars allow the wings to achieve omnidirectional and broadband antireflection properties. Another type of clear wing butterfly is a longtail glasswing (Chorinea faunus) which has dome-shaped nanopillars with a moderate aspect ratio $(1.090 \pm 0.041)^{[89]}$ as shown in Figure 5 (right). One study describes the use of strong anti-reflective structures inspired by Longtail Glasswing Butterfly in one stage of material processing.^[54] Scientists have obtained sub-wavelength structures of silica with an arbitrary distance of 80/130/180 nm, partially embedded in a polymer matrix, creating a gradual refractive index transition at the air/substrate interface to suppress light reflection. It is important to note that randomly spaced sub-wavelength silica colloids show even better anti-reflection characteristics at high angles of incidence than 2D loosely packed colloidal silica crystals.[88,90,91]

2.5. Chitin Nanofiber (CHINF)

Crustaceans offer great prospects in the research of anti-reflective properties. Chitin nanofibers (CHINF) are the most often used (SEM image shown in Figure 6). A scientific paper published last year by Keio University, Japan, shows that durable thin films with low refractive index and anti-reflective properties were successfully manufactured using chitin nanofibers obtained from crab shells. A film with a low refractive index was obtained by forming porous thin films; porosity was obtained by increasing the number of air spaces inside the membrane. To achieve the effective laying of CHINF, the layer-by-layer method (LBL) was used. The effect of the surface structure and refractive index on the change in the pH of the solution was studied using scanning electron microscopy and ellipsometry. The transmittance of the fabricated film is 4.1% higher than that of a glass substrate and the refractive index film of that is 1.29. The films had abrasion resistance and antifogging properties because of the high mechanical strength and hydrophilicity of chitin. We believe that LBL film, using CHINF, is a promising candidate material to be used in overcoming the durability problems associated with optical thin films.[92-96]

3. Future Direction

Nature is vast and diverse in its manifestations—and much more research is needed. In the following sections, we will describe insects and deep-sea inhabitants that have sub-wavelength structures but have not yet been studied from the aspect of anti-reflective surfaces. Specifically, we will review the creatures dwelling in the deep sea. These organisms possess sub-wavelength structures that have not yet been thoroughly examined for their potential in anti-reflective techniques.

3.1. Tortoise Beetle

Charidotella ambita is a beetle whose elytral surface color changes depending on the stage of mating behavior (color changes from dull red to "goldish"), as shown in **Figure 7**. Its properties are being investigated to understand the origin of the "goldish" surface color, but its ability to turn golden and then matte is still puzzling. As can be seen from Figure 7B,C, the beetle does not have sub-wavelength structures. Its golden reflector is a multi-layer structure consisting of up to 50 alternating bilayers of high and low density, parallel to the cuticle surface. These properties result from different structures, that is, diffraction gratings, multilayer or 3D photonic crystals located in the upper layers of the epidermis. In this case, the color change is associated with a multilayer structure and fluid movement. [97]

3.2. Shrimps

Shrimp is a good example of a crustacean whose chitin can be used to produce anti-reflective surfaces. Chitin nanofibers obtained from crab shells are already used for the production of anti-reflective films. But in nature, there is a large variety of crustacean chitin with anti-reflective properties. Chitin itself is a waste product of the shrimp industry. It is environmentally safe, economically profitable, easy to use, and does not require long multi-stage processes to produce chitin films. For example, in one of the studies, reflective films of a chitin nature were studied. It was found that films obtained from shrimp chitin powder have a low reflectivity of ChNC (less than one percent), which confirms that chitin has an anti-reflective property, so there is no need to process it before usage. [98]

nditions) on Wiley Online Library for rules of use; OA articles are governed by the applicable Creative Commons

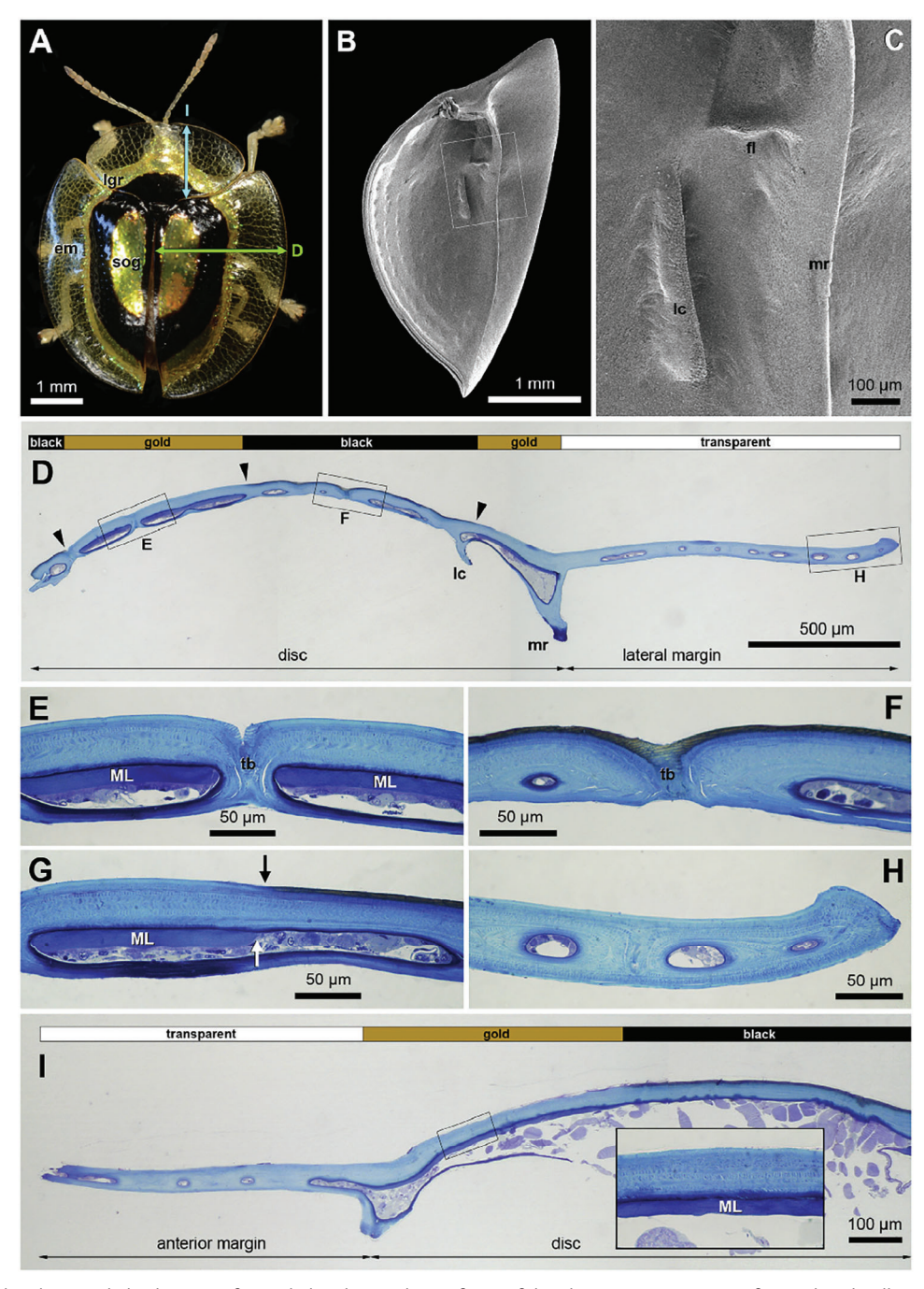


Figure 7. Tortoise beetle. A) A light drawing of a turtle beetle. B) The surfaces of the elytra. C) SEM image of (A). Charidotella ambit habitus at 100-fold magnification. D) Light microscopy of the lateral edge of the sample. E) Light microscopy of region E. F) Light microscopy of region F. G) Light microscopy of region G. H) Light microscopy of region H. I) SEM image of the leading edge of the sample. Reproduced with permission.^[97] Copyright 2016, Elsevier.

3.3. Hermetia Illucens

Hermetia Illucens or black soldier fly is a species of Diptera from the Stratiomyidae family. The bodies of the flies are completely black and opaque and do not reflect light, which makes them interesting for the study of anti-reflective surfaces. **Figure 8** shows that the surfaces of black soldier fly bodies include several types of sub-wavelength structures, namely repeating square, pentagonal, and hexagonal units, mixed together. These types of structures are located on the same surface of the fly body and their repeatability and location depend on the age of the fly. These sub-wavelength structures are already separately used to create anti-reflection layers—that is, only square units, or only hexagonal patterns—but have never been studied as an array.

2365709x, 2024, 2, Downloaded from https://advanced.onlinelibrary.wiley.com/doi/10.1002/admt.202301128 by Ben Gurion University, Wiley Online Library on [23/10/2025]. See the Terms

ditions) on Wiley Online Library for rules of use; OA articles are governed by the applicable Creative Commons

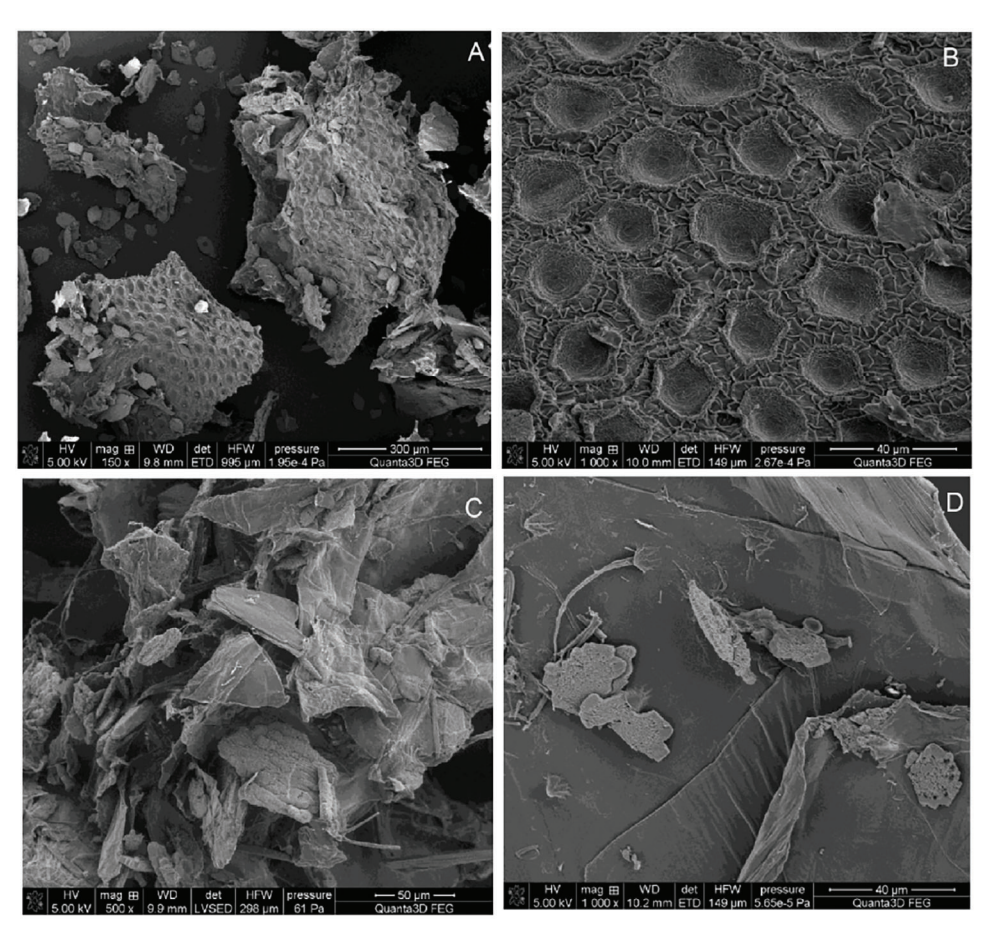


Figure 8. SEM images of different parts of chitins isolated from A) pupal exuviae and B) image with magnification of C) \times 500 and D) \times 1000. Reproduced with permission. [99] Copyright 2016, Elsevier.

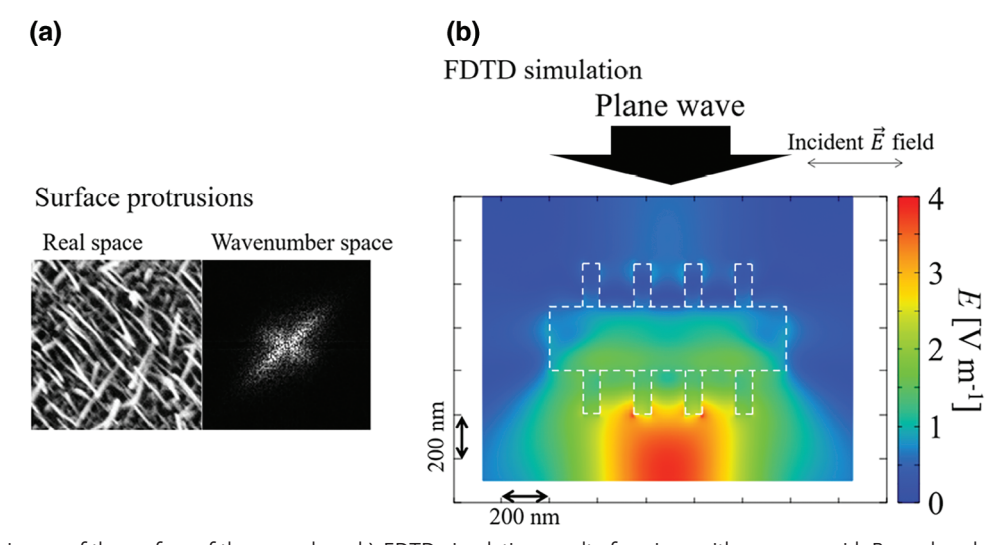


Figure 9. a) SEM image of the surface of the green lace. b) FDTD simulation results for wings with a square grid. Reproduced with permission.^[101] Copyright 2022, American Chemical Society.

Wiley Online Library on [23/10/2025]. See

conditions) on Wiley Online Library for rules of use; OA articles are governed by the applicable Creative Comi

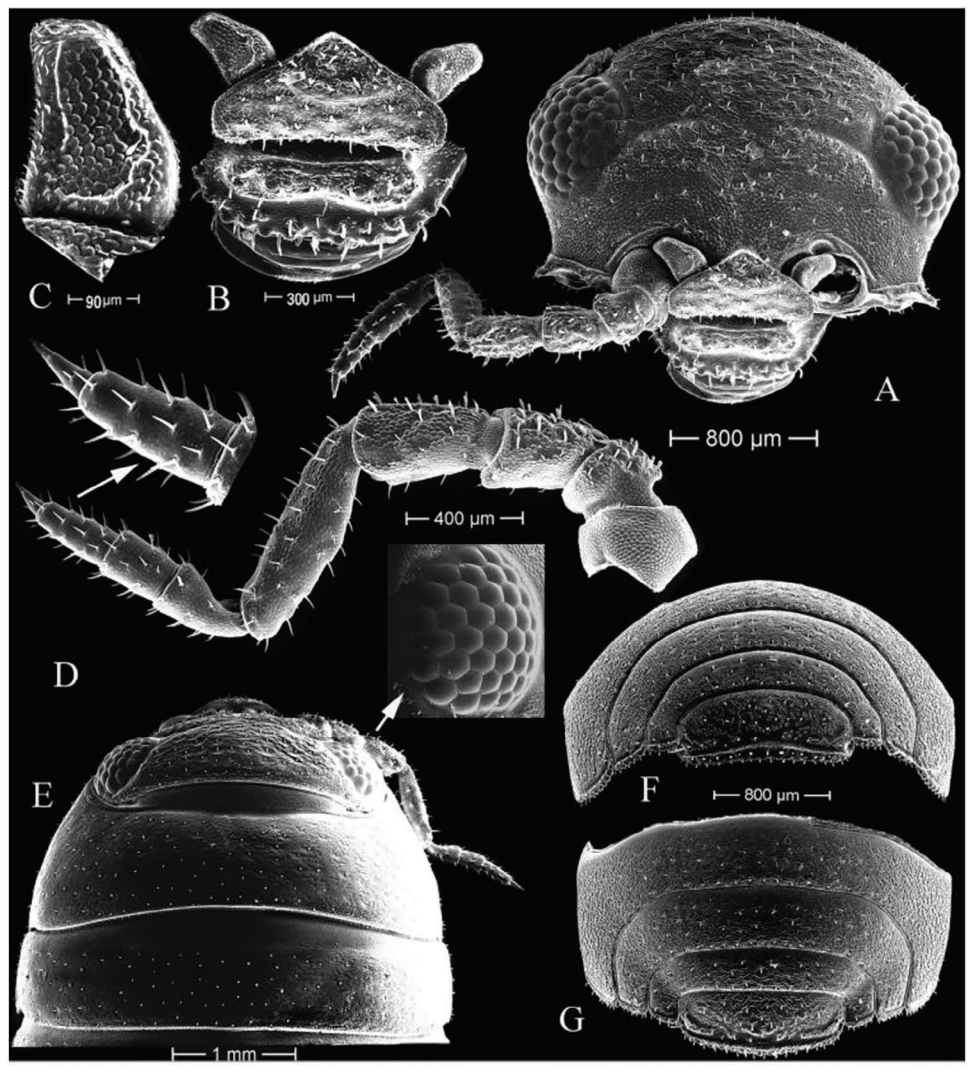


Figure 10. A-G) SEM image of body parts of Tylosmaindroni Giordani Soika. Reproduced with permission. [102] Copyright 2022, Pensoft Publishers.

3.4. Green Lacewings

Green lacewings belong to the family Chrysopidae and are found widespread throughout North America. The surfaces of their wings do not reflect light. It was found that these surfaces consist of projections arranged in the form of a square grid on the base substrate, in a cross-shaped pattern. **Figure 9** shows that this is a repeating pattern, but chaotic; nevertheless, it belongs to subwavelength structures. The results of modeling patterns on the substrate show that the surface projections of the wing increase the intensity of the transmitted light and decrease the intensity of the reflected light, respectively. This phenomenon has also been observed in the case of incident light at an angle of 45°.[101]

3.5. Woodlouse

A type of crustacean with chitinous non-reflective coating shells, the woodlouse, belongs to the suborder Oniscidea of the Isopoda

order. It gets its name because it can often be found in old wood. The optical properties of the shells have not yet been studied, so they may present a prospect for research. A scanning electron microscopy image in **Figure 10** shows a species of woodlouse, Tylosmaindroni Giordani Soika. A variety of periodic structures are located on different parts of the body, at the same distance from one another. The structural forms are spherical, porous, and conical sub-wavelength structures, as well as cylindrical structures connected in a row of 3–4 cylinders and located in the same direction. On some surfaces, several sub-wavelength structures appear at once, most likely due to other properties in addition to anti-reflection.

3.6. Grasshopper

Figure 11a shows the surfaces of a nymph, and Figure 11b the adult individuals of Dociostaurus maroccanus, or its other name, Grasshopper.^[103] Chitins extracted from adult grasshoppers and

doi/10.1002/admt.202301128 by Ben Gurion

Wiley Online Library on [23/10/2025]. See

onditions) on Wiley Online Library for rules of use; OA articles are governed by the

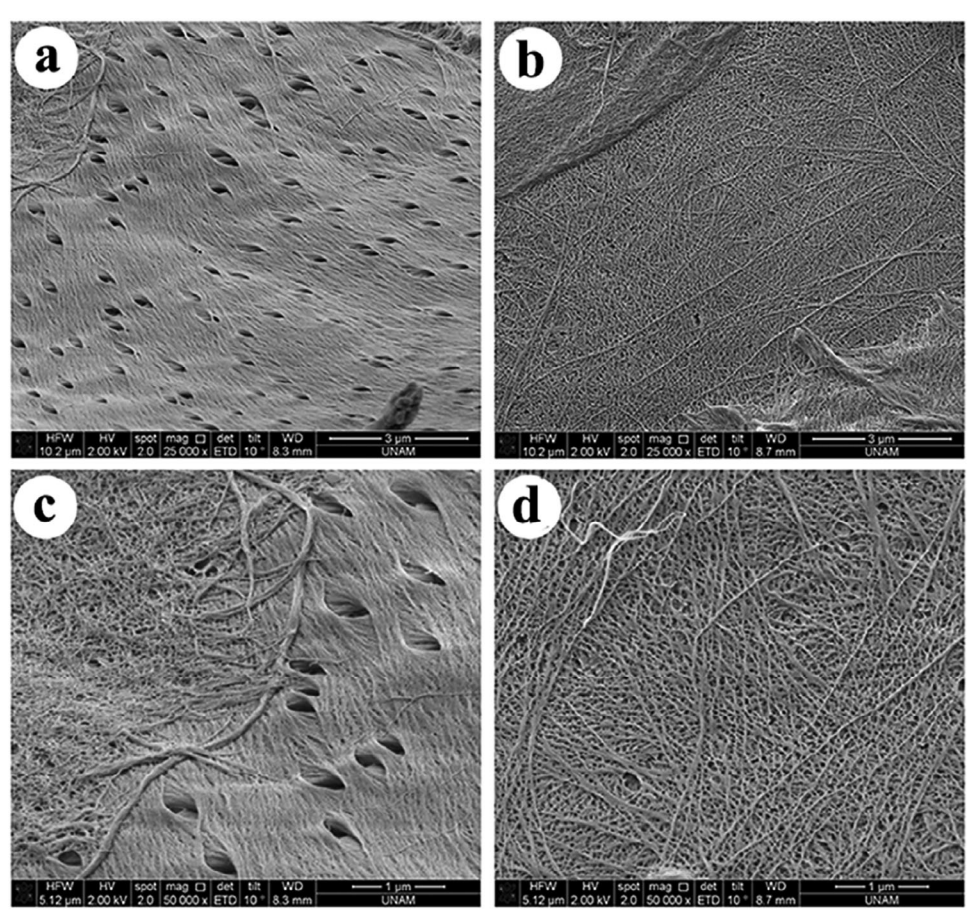


Figure 11. SEM images of grasshopper chitins and chitosans. a) Chitin of adult individuals, b) chitosan of adult individuals, c) chitin of nymphs, and d) chitosan of nymphs. Reproduced with permission.^[103] Copyright 2016, Elsevier.

nymphs consist of elongated and well-packed nanofibers, neatly stacked one after another and randomly scattered in large nanopores about 200 nm in size. These differ from the chitin wrapping in crustaceans (Figure 6), where the filaments are of different thicknesses and are arranged randomly. The nanopores densely observed on the surface of chitin are known as pore channels, which serve to transport ions and nutrients from the hypodermis to the inner epicuticle and stitch the structure together. In this case, we can assume that a mixture of sub-wavelength structures is presented here, consisting of tightly packed nanofibers and pores.

4. Conclusion

Sub-wavelength structures of marine species and insects are very popular in the field of optics because they possess interesting optical properties observed in nature. The structures are cone-shaped lattices symmetrically and asymmetrically located, multi-layer nanostructures with pores, and other forms. Different sub-wavelength structures have different reflection coefficients. Their reflections can be in different wavelength ranges. It should also be noted that all the main sub-wavelength structures are represented by living organisms that have chitin in their cell walls;

therefore, research should be developed in the field of utilizing chitin surfaces to reduce light reflection. Several sub-wavelength geometries can work efficiently on the same surface simultaneously. The basis of all these structures is an affordable and environmentally friendly material, namely, chitin. Chitin can perhaps be used for a variety of anti-reflective coatings, including solar panels.

Acknowledgements

The research leading to the results was supported by EU ERA-NET DIEGO project, Ministry of Energy, Grant No. 221-11-032 and the School of Sustainable Development and Climate Change (SSCC) of Ben-Gurion University of the Negev.

Conflict of Interest

The authors declare no conflict of interest.

Keywords

anti-reflection coatings, anti-reflection surfaces, biomimicry, solar cells, sub-wavelength structures

and Conditions

onditions) on Wiley Online Library for rules of use; OA articles are governed by the applicable Creative Common

Received: July 9, 2023 Revised: October 2, 2023 Published online: November 27, 2023

- ____
- 2022, 1002, 012008.
 [2] E. M. Sunderland, C. T. Driscoll Jr, J. K. Hammitt, P. Grandjean, J. S. Evans, J. D. Blum, C. Y. Chen, D. C. Evers, D. A. Jaffe, R. P. Mason, S. Goho, W. Jacobs, *Environ. Sci. Technol.* 2016, 50, 2117.

[1] R. M. Hannun, A. H. A. Razzaq, IOP Conf. Ser.: Earth Environ. Sci.

- [3] D. Pudasainee, J.-H. Kim, S.-H. Lee, J.-M. Park, H.-N. Jang, G.-J. Song, Y.-C. Seo, Asia-Pac. J. Chem. Eng. 2010, 5, 299.
- [4] A.-E. Becquerel, C. R. Acad. Sci. 1839, 9, 145.
- [5] D. M. Chapin, C. S. Fuller, G. L. Pearson, J. Appl. Phys. 1954, 25, 676.
- [6] B. K. Nayak, V. V. Iyengar, M. C. Gupta, Prog. Photovoltaics 2011, 19, 631.
- [7] J. Moghal, S. Reid, L. Hagerty, M. Gardener, G. Wakefield, Thin Solid Films 2013, 534, 541.
- [8] S. Y. Ekinci, S. Sancakli, L. Adam, J. M. Walls, J. Energy Syst. 2022, 6, 33.
- [9] H. K. Raut, V. A. Ganesh, A. S. Nair, S. Ramakrishna, Energy Environ. Sci. 2011, 4, 3779.
- [10] P. Xiao, M. Zhang, X. Wu, K. Ding, J. Pan, J. Jie, Solar Energy 2022, 234, 111.
- [11] M. A. Zahid, M. Q. Khokhar, S. Park, S. Q. Hussain, Y. Kim, J. Yi, Vacuum 2022, 200, 110967.
- [12] W. Zhang, K. Hu, J. Tu, A. Aierken, D. Xu, G. Song, X. Sun, L. Li, K. Chen, D. Zhang, Y. Zhuang, P. Xu, H. Wu, Solar Energy 2021, 217, 271
- [13] A. J. Addie, R. A. Ismail, M. A. Mohammed, Sci. Rep. 2022, 12, 9902.
- [14] P. A. M. Mercy, K. J. Wilson, Mater. Today: Proc. 2022, 64, 1778.
- [15] S. Chattopadhyay, Y.-F. Huang, Y.-J. Jen, A. Ganguly, K. Chen, L. Chen, Mater. Sci. Eng., R 2010, 69, 1.
- [16] C. Striemer, P. Fauchet, Appl. Phys. Lett. 2002, 81, 2980.
- [17] K. Askar, B. M. Phillips, Y. Fang, B. Choi, N. Gozubenli, P. Jiang, B. Jiang, Colloids Surf. A 2013, 439, 84.
- [18] C. M. Soukoulis, S. Linden, M. Wegener, Science 2007, 315, 47.
- [19] C. Bernhard, W. H. Miller, Acta Physiol. Scand. 1962, 56, 385.
- [20] S.-W. Ahn, K.-D. Lee, J.-S. Kim, S. H. Kim, J.-D. Park, S.-H. Lee, P.-W. Yoon, *Nanotechnology* 2005, 16, 1874.
- [21] T. Siefke, S. Kroker, K. Pfeiffer, O. Puffky, K. Dietrich, D. Franta, I. Ohlídal, A. Szeghalmi, E.-B. Kley, A. Tünnermann, Adv. Opt. Mater. 2016. 4, 1780.
- [22] T. Ang, G. Reed, A. Vonsovici, A. Evans, P. Routley, M. Josey, IEEE Photonics Technol. Lett. 2000, 12, 59.
- [23] D. Taillaert, F. Van Laere, M. Ayre, W. Bogaerts, D. Van Thourhout, P. Bienstman, R. Baets, Jpn. J. Appl. Phys. 2006, 45, 6071.
- [24] Y. Galutin, E. Falek, A. Karabchevsky, Sci. Rep. 2017, 7, 12076.
- [25] S. M. Rytov, Sov. Phys. JETP 1956, 2, 466.
- [26] G. Beadie, J. S. Shirk, A. Rosenberg, P. A. Lane, E. Fleet, A. Kamdar, Y. Jin, M. Ponting, T. Kazmierczak, Y. Yang, A. Hiltner, E. Baer, Opt. Express 2008, 16, 11540.
- [27] H. Wang, F. Zhang, C. Wang, J. Duan, Opt. Laser Technol. 2022, 149, 107931.
- [28] T. Muratsubaki, T. Fujisawa, Y. Sawada, T. Sato, K. Saitoh, Jpn. J. Appl. Phys. 2022, 61, 042003.
- [29] X. Wang, Y. Ren, T. Jia, Y. Su, Y. Qi, X. Wen, Mod. Phys. Lett. B 2022, 36, 2150553.
- [30] T. Jia, Y. Ren, X. Wang, Y. Qi, X. Wen, Opt. Quantum Electron. 2022, 54, 208.
- [31] I. Staude, J. Schilling, Nat. Photonics 2017, 11, 274.
- [32] J. S. Choi, Y.-W. Jang, U. Kim, M. Choi, S. M. Kang, Adv. Energy Mater. **2022**, *12*, 2201520.

- [33] Y. Liu, Y. Wang, M. Yang, Q. Wu, Z. Li, C. Zhang, J. Zhang, J. Yao, J. Xu, Appl. Surf. Sci. 2022, 573, 151576.
- [34] Y. Wang, W. Huang, Y.-S. Lin, B.-R. Yang, Nanoscale Adv. 2022, 4, 3624.
- [35] H. J. Brunner, J. Whitehead, R. Gibson, J. R. Hendrickson, A. Majumdar, J. D. MacKenzie, Adv. Mater. Interfaces 2022, 9, 2200149.
- [36] A. Jacobo-Martín, J. J. Hernández, E. Solano, M. A. Monclús, J. C. Martínez, D. F. Fernandes, P. Pedraz, J. M. Molina-Aldareguia, T. Kubart, I. Rodríguez, Appl. Surf. Sci. 2022, 585, 152653.
- [37] A. Naser, D. Hachim, Q. Abed, presented at Proc. 2nd Int. Multi-Disciplinary Conf. Theme: Integrated Sciences and Technologies, IMDC-IST, Sakarya, Turkey, September 2022.
- [38] M. Wang, H. He, C. Shou, H. Cui, D. Yang, L. Wang, Mater. Sci. Semicond. Process. 2022, 138, 106299.
- [39] A. Karabchevsky, E. Falek, Y. Greenberg, M. Elman, Y. Keren, I. Gurwich, Nanoscale Adv. 2020, 2, 2977.
- [40] E. Falek, A. Katiyi, Y. Greenberg, A. Karabchevsky, Adv. Opt. Mater. 2021, 9, 2100130.
- [41] A. Karabchevsky, A. Katiyi, A. S. Ang, A. Hazan, Nanophotonics 2020, 9, 3733.
- [42] H. Kikuta, H. Toyota, W. Yu, Opt. Rev. 2003, 10, 63.
- [43] C.-H. Sun, P. Jiang, B. Jiang, Appl. Phys. Lett. 2008, 92, 061112.
- [44] H. Lin, M. Ouyang, B. Chen, Q. Zhu, J. Wu, N. Lou, L. Dong, Z. Wang, Y. Fu, Coatings 2018, 8, 360.
- [45] R. Brunner, O. Sandfuchs, C. Pacholski, C. Morhard, J. Spatz, Laser Photonics Rev. 2012, 6, 641.
- [46] C. Hua, Z. Cheng, Y. Ma, H. He, G. Xu, Y. Liu, S. Yang, G. Han, J. Electrochem. Soc. 2021, 168, 042503.
- [47] M.-S. Shih, H.-Y. Chen, P.-C. Li, H. Yang, Appl. Surf. Sci. 2020, 532, 147397
- [48] S. Dou, H. Xu, J. Zhao, K. Zhang, N. Li, Y. Lin, L. Pan, Y. Li, Adv. Mater. 2021, 33, 2000697.
- [49] C.-W. Lei, R.-Y. Chen, H. Yang, Langmuir 2020, 36, 5296.
- [50] Z. Li, Q. Yan, Y. Qin, W. Kong, G. Li, M. Zou, D. Wang, Z. You, X. Zhou, Opt. Express 2019, 27, 702.
- [51] Y. Zhang, C. Li, M. Loncar, Opt. Lett. 2013, 38, 646.
- [52] L. Wu, J. He, W. Shang, T. Deng, J. Gu, H. Su, Q. Liu, W. Zhang, D. Zhang, Adv. Opt. Mater. 2016, 4, 195.
- [53] S. Haghanifar, M. McCourt, B. Cheng, J. Wuenschell, P. Ohodnicki, P. W. Leu, *Mater. Horiz.* 2019, 6, 1632.
- [54] C.-J. Lai, H.-P. Tsai, J.-Y. Chen, M.-X. Wu, Y.-J. Chen, K.-Y. Lin, H.-T. Yang, Nanomaterials 2022, 12, 1856.
- [55] Z. Jakšić, D. Pantelić, M. Sarajlić, S. Savić-Šević, J. Matović, B. Jelenković, D. Vasiljević-Radović, S. Ćurčić, S. Vuković, V. Pavlović, J. Buha, V. Lačković, M. Labudović-Borović, B. Ćurčić, *Opt. Mater.* 2013, 35, 1869.
- [56] S. Suenaga, M. Osada, Cellulose 2018, 25, 6873.
- [57] S. Ifuku, Z. Shervani, H. Saimoto, in *Biopolymer Nanocomposites: Processing, Properties, and Applications* (Eds: A. Dufresne, S. Thomas, L. A. Pothen), Wiley, Hoboken, NJ 2013, Ch. 2.
- [58] E. Lizundia, T.-D. Nguyen, R. J. Winnick, M. J. MacLachlan, J. Mater. Chem. C 2021, 9, 796.
- [59] S. Luke, P. Vukusic, Europhys. News 2011, 42, 20.
- [60] Y.-K. Lin, Y.-S. Chen, C.-H. Hsueh, Results Phys. 2019, 12, 244.
- [61] M. Kengo, T. Chie, M. Yukari, T. Mizuki, N. Chiaki, T. Yuki, M. Takeshi, K. Kyu-Hong, S. Seimei, ACS Appl. Mater. Interfaces 2016, 8, 31951.
- [62] H. Lee, A. Yi, J. Choi, D.-H. Ko, H. J. Kim, Appl. Surf. Sci. 2022, 584, 152625.
- [63] S. Li, X. Wu, J. Duan, S. Yuan, C. Wang, Y. Ma, Z. Zhang, Shock Vib. 2021, 2021, 1480264.
- [64] T. Lv, Y. Tang, H. Fan, S. Liu, S. Zeng, W. Liu, Sol. Energy Mater. Sol. Cells 2022, 235, 111450.
- [65] A. S. Rad, A. Afshar, M. Azadeh, Opt. Mater. 2020, 107, 110027.

www.advmattechnol.de

www.advancedsciencenews.com

- [66] N. Rezaei, O. Isabella, Z. Vroon, M. Zeman, Solar Energy 2019, 177, 59
- [67] W.-K. Kuo, J.-J. Hsu, C.-K. Nien, H. H. Yu, ACS Appl. Mater. Interfaces 2016. 8, 32021.
- [68] G. Han, T.-B. Nguyen, S. Park, Y. Jung, J. Lee, H. Lim, ACS Nano 2020, 14, 10198.
- [69] S. Wilson, M. Hutley, Opt. Acta 1982, 29, 993.
- [70] C. G. Bernhard, Endeavour 1967, 26, 79.
- [71] P. Clapham, M. Hutley, Nature 1973, 244, 281.
- [72] S.-H. Nam, J.-H. Boo, Energy Rep. 2022, 8, 98.
- [73] R. R. Alfarah, A. J. Boukar, A. M. Algnoni, in 2022 IEEE 2nd Int. Maghreb Meeting of the Conf. on Sciences and Techniques of Automatic Control and Computer Engineering (MI-STA), IEEE, Piscataway, NJ 2022, pp. 640–644.
- [74] T. Yanagishita, M. Omata, H. Masuda, Jpn. J. Appl. Phys. 2022, 61, 038001.
- [75] S. Yang, N. Sun, B. B. Stogin, J. Wang, Y. Huang, T.-S. Wong, *Nat. Commun.* 2017, 8, 1285.
- [76] A. Yoshida, M. Motoyama, A. Kosaku, K. Miyamoto, Zool. Sci. 1997, 14, 737.
- [77] I. R. Hooper, P. Vukusic, R. Wootton, Opt. Express 2006, 14, 4891.
- [78] M. Day, M. Briggs, J. Ultrastruct. Res. 1958, 2, 239.
- [79] R. A. Rakitov, Zool. J. Linn. Soc. 2004, 140, 353.
- [80] H.-Y. Chen, K.-T. Chiang, Y.-Z. Ye, K.-Y. A. Lin, H. Yang, J. Taiwan Inst. Chem. Eng. 2022, 136, 104407.
- [81] Z. Jakšić, M. Obradov, O. Jakšić, D. Tanasković, Opt. Quantum Electron. 2022, 54, 524.
- [82] Y. Si, T. Huang, H. Xie, M. Chen, Chem. Mater. 2022, 34, 7271.
- [83] W. Cai, Z. Li, T. Cui, X. Feng, L. Song, Y. Hu, X. Wang, Composites, Part B 2022, 244, 110204.
- [84] H.-Y. Tseng, Y.-H. Chen, R.-Y. Chen, H. Yang, ACS Appl. Mater. Interfaces 2020, 12, 10883.
- [85] R.-Y. Chen, C.-J. Lai, Y.-J. Chen, M.-X. Wu, H. Yang, J. Colloid Interface Sci. 2022, 610, 246.
- [86] H. Ding, B. Li, Z. Wang, S. Niu, Z. Han, L. Ren, *Matter* **2022**, *5*,

- [87] S. R. Mouchet, C. Verstraete, B. Bokic, D. Mara, L. Dellieu, A. G. Orr, O. Deparis, R. Van Deun, T. Verbiest, P. Vukusic, B. Kolaric, J. Lumin. 2023. 254. 119490.
- [88] R. H. Siddique, G. Gomard, H. Hölscher, Nat. Commun. 2015, 6, 6909
- [89] V. Narasimhan, R. H. Siddique, J. O. Lee, S. Kumar, B. Ndjamen, J. Du, N. Hong, D. Sretavan, H. Choo, Nat. Nanotechnol. 2018, 13, 512.
- [90] V. Narasimhan, R. H. Siddique, Y. M. Wang, H. Choo, in 2022 IEEE 35th Int. Conf. on Micro Electro Mechanical Systems (MEMS), IEEE, Piscataway, NJ 2022, pp. 25–26.
- [91] A. F. Pomerantz, R. H. Siddique, E. I. Cash, Y. Kishi, C. Pinna, K. Hammar, D. Gomez, M. Elias, N. H. Patel, bioRxiv, Dev. Biol. 2020, doi: https://doi.org/10.1101/2020.11.30.404111.
- [92] C. Tanaka, S. Shiratori, MATEC Web Conf. 2013, 4, 05006.
- [93] L. Bai, L. Liu, M. Esquivel, B. L. Tardy, S. Huan, X. Niu, S. Liu, G. Yang, Y. Fan, O. J. Rojas, Chem. Rev. 2022, 122, 11604.
- [94] H. Gong, S. Luo, H. Li, S. Liu, Mater. Technol. 2022, 37, 1989.
- [95] S. Thomas, B. Seufert, W. Serrano-Garcia, M. Devisetty, R. Khan, K. Puttananjegowda, N. Alcantar, Sustainable Nanotechnology: Strategies, Products, and Applications, Wiley, Hoboken, NJ 2022, p. 173.
- [96] J. Hou, B. E. Aydemir, A. G. Dumanli, *Philos. Trans. R. Soc., A* 2021, 379, 20200331.
- [97] J. M. Pasteels, O. Deparis, S. R. Mouchet, D. M. Windsor, J. Billen, Arthropod Struct. Dev. 2016, 45, 509.
- [98] A. Narkevicius, R. M. Parker, J. Ferrer-Orri, T. G. Parton, Z. Lu, G. T. van de Kerkhof, B. Frka-Petesic, S. Vignolini, Adv. Mater. 2022, 34, 2203300
- [99] A. Waśko, P. Bulak, M. Polak-Berecka, K. Nowak, C. Polakowski, A. Bieganowski, Int. J. Biol. Macromol. 2016, 92, 316.
- [100] P. Weththasinghe, J. Ø. Hansen, L. T. Mydland, M. Øverland, Rev. Aquacult. 2022, 14, 938.
- [101] K. Yoshida, Y. Katsurashima, L. Takahashi, Langmuir 2022, 38, 3098.
- [102] V. Khalaji-Pirbalouty, H. Oraie, C. A. Santamaria, J. W. Wägele, ZooKeys 2022, 1087, 123.
- [103] S. Erdogan, M. Kaya, Int. J. Biol. Macromol. 2016, 89, 118.



Anastasia Novikova received a BSc degree in Environmental protection at the Tomsk Polytechnic University in 2014, and a master's degree in Biotechnological Engineering at the Tomsk Polytechnic University in 2016. She was awarded the Tomsk University student's award to visit the Light-on-a-Chip group in 2019. In 2020, Anastasia was accepted as a Ph.D. student at the School of Electrical and Computer Engineering at BGU. Her research interests are in nanoparticles, composite sorbents, water purification, toxic pollution, waveguides, sensing, optical fiber, sensors, solar cells, and quantum dots.



Dr. Aviad Katiyi obtained his B.Sc. in Electrooptical Engineering from the Lev Institute of Jerusalem in 2013. In 2017 and 2021 Aviad obtained his M.Sc. and Ph.D. respectively in Photonics and Electro-Optics Engineering at Ben-Gurion University under the supervision of Prof. Karabchevsky. His main interests lie in the areas of guided-wave optics.



Prof. Alina Karabchevsky is an Associate Professor at the School of Electrical and Computer Engineering at Ben-Gurion University of the Negev (BGU) and the Chair of IEEE Women in Engineering Affinity Group (Israel Section). She is the Head of the Light-on-a-Chip center at the BGU. Her main research interests lie in the areas of integrated photonics and microfibers, all-dielectric photonics, plasmonics, microfluidics and optomechanics.